Accepted to Phys. Fluids 10.1063/5.0132565

Nuclear Explosion Impact on Humans Indoors

Ioannis W. Kokkinakis[1, a)] and Dimitris Drikakis[1, b)]
University of Nicosia, Nicosia CY-2417, Cyprus

(Dated: 24 November 2022)

The nuclear blast effects on humans inside a building within the moderate damage zone (MDZ) are investigated. These effects depend on many parameters that must be better understood. Injuries will spread further away than the devastating destruction zone, where most people are killed instantly. Still, these injuries will vary depending on a person's position in the building and the air velocities attained when the blast wave enters indoors. The blast wave effects are examined for an indicative, easily reproducible indoor arrangement. The airspeed behind the blast wave accelerates to even higher velocities in the interior. The supersonic shock waves arising from the blast undergo expansion as they enter a room through an opening leading to channelling effects. The results show that most of the air is directed towards the corridor rather than through the opposite room's door, leading to high airspeed developed in rooms further down the aisle. The airspeed attained in the interior is calculated for two blast wave overpressures, 3 and 5 pounds per square inch (psi), for which most concrete buildings do not collapse. The data reveals that the force applied to a standing person from the speed of the gusts formed at several locations in the interior is equivalent to several $g-$forces of body mass acceleration capable of lifting and throwing any person off the ground. It is then the impact onto solid surfaces that can lead to severe injury or death. Finally, the results reveal preferential areas in the rooms where a human can avoid the risk of exposure to the highest wind forces.

I. INTRODUCTION

The detonation of a nuclear bomb will have devastating effects on humans and assets. The shock waves and thermal and ionizing radiation will cause destruction. Moreover, radioactive fallout will impact for years. The shock waves will cause most of the damage through fast changes in air pressure that will destroy people, trees and manufactured structures. The destruction will depend on the magnitude of the explosion, and the greater the distance one wants to achieve, the greater the burst height should be. Air bursts will result in higher overpressures at longer distances. In contrast, surface explosions will lead to higher overpressures at closer distances.

Although estimating the various effects at different distances is complicated, a general assessment based on past nuclear tests and engineering projections suggests that overpressures at and above 20 pounds per square inch (psi) will partially or entirely demolish heavily concrete buildings[1–3]. At 10 psi, most people will die, and severe damage will occur. At 5 psi, severe injuries and fatalities to humans will be widespread and significant damage to heavy structures will occur. Finally, at longer distances featuring 3 psi, overpressure will result in severe human injuries, and the destruction of smaller built-in structures[3]. For the range of overpressures below 5 psi, humans outdoors will be exposed to the absolute risk of severe injury or death. The blast waves, debris from structures, radiation and nuclear fallout will cause the above.

Several studies in the past have simulated the dispersion and deposition of radioactive fallout from nuclear tests[4,5] or terrorist nuclear detonations[6–8] and modeled the radioactive fallout from stabilized nuclear clouds[9] and atomic weapon tests[10]. Obviously, near the nuclear bomb detonation, the devastation would be widespread, and the fatality rate would be practically 100%. However, outside of the severe damage zone (SDZ), the effect of the blast reduces and survivability increases. Severe injuries can be reduced at distances corresponding to overpressures below 5 psi, particularly for people inside concrete buildings within the moderate damage zone (MDZ). In this case, the primary danger to human survivability in indoor spaces becomes the extreme high-speed winds that enter through the various openings in the building, e.g., windows. In addition, the propagation of shock waves indoors will interact with walls and deflect around corners, doors and obstacles. These interactions may induce higher pressures due to channelling effects, thus increasing the injury risk.

The problem is multiparametric, as indoor spaces vary regarding obstacles and architectural layout. Thus the details of the phenomena will be indoor arrangement dependent. Despite that, significant conclusions can be drawn from the induced forces, which can help minimize the effect of blast impact. This study shows that in the range of nuclear explosion far-field overpressures below 5 psi, the injury for people indoors can vary and be reduced depending on the position of humans in the building.

Tactical nuclear weapons range between 5 and 15 kilotons (kT). In the present study, however, we have chosen a 750 kT atomic warhead as this corresponds to an extreme scenario of an upper range value of a multiple independently targetable reentry vehicle, such as, for example, the RS-28 Sarmat (Satan II)[11]. Of course, this scenario is unthinkable, but it represents a catastrophic scenario due to the existence of such a warhead and the increasing geopolitical tensions. Therefore, we aim to alert the world through rigorous scientific simulations of the impact of such a scenario, particularly in MDZ. To our knowledge, no previous studies have examined the risk to humans caused by the high-speed winds from nuclear blasts entering buildings within the MDZ.

Section § II provides a brief description of the computational methodology. Section § III describes (i) the computational setup used to simulate the nuclear blast § III A, (ii) the

[a)]Electronic mail: kokkinakis.i@unic.ac.cy
[b)]Electronic mail: Corresponding author, drikakis.d@unic.ac.cy

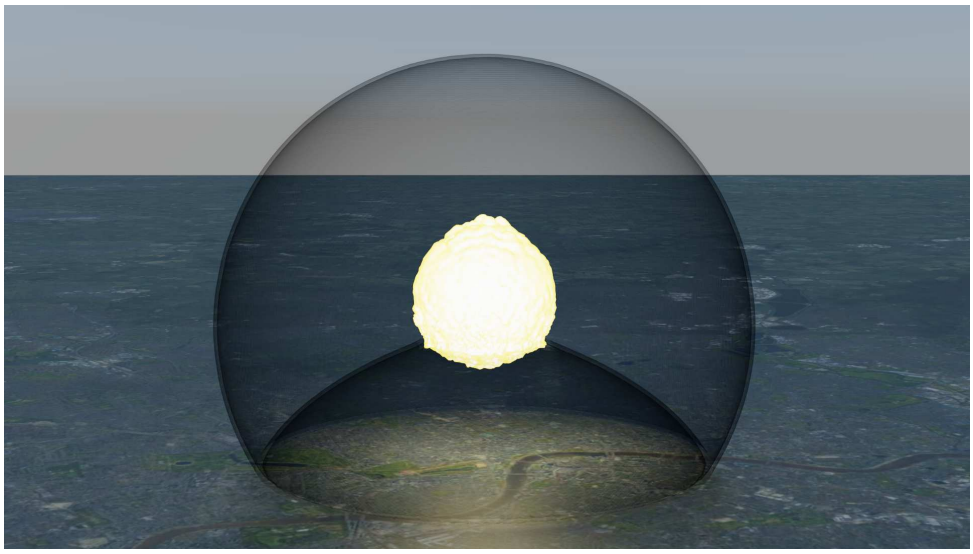

FIG. 1. Three-dimensional illustration of the air blast and generated blast wave 10 seconds following the detonation of a 750 kT nuclear warhead above a typical metropolitan city; the radius of the shock bubble at ground level is 4.6 km with a peak overpressure of slightly over 7 psi.

equations for modeling the blast wave at the building windows § III B, (iii) the layout and dimensions of a (simplified) model room layout § III C, and (iv) the calculation of the force on a human §III D. In Section § IV, we present the simulation results obtained for the considered nuclear blast scenario of a 750 kT atomic warhead §IV A and establish the hazard imposed to humans indoors within the MDZ §IV B. Finally, in section § V, we summarize the main findings drawn from this study.

II. COMPUTATIONAL METHODOLOGY

We solve the compressible Euler equations for an ideal gas using the finite volume method (FVM). In integral form, the equations are formulated as follows:

$$\frac{\partial}{\partial t}\iiint_V \rho \,\mathrm{dV} = -\oiint_A \rho \mathbf{u}\cdot\hat{\mathbf{n}}\,\mathrm{dA} \tag{1}$$

$$\begin{aligned}\frac{\partial}{\partial t}\iiint_V \rho\mathbf{u}\,\mathrm{dV} = &-\oiint_A (\rho\mathbf{u}\mathbf{u}+p\mathrm{I})\cdot\hat{\mathbf{n}}\,\mathrm{dA}\\ &+\iiint_V \rho\mathbf{f}_b\,\mathrm{dV}\end{aligned} \tag{2}$$

$$\begin{aligned}\frac{\partial}{\partial t}\iiint_V \rho e_t\,\mathrm{dV} = &-\oiint_A (\rho e_t + p)\,\mathbf{u}\cdot\hat{\mathbf{n}}\,\mathrm{dA}\\ &+\iiint_V \rho\mathbf{f}_b\cdot\mathbf{u}\,\mathrm{dV}\end{aligned} \tag{3}$$

where ρ is the density; $\mathbf{u}$ is the velocity vector; p is the static pressure; $\hat{\mathbf{n}}$ is the outward pointing unit normal of a surface element dA of the closed finite control volume dV; $\mathbf{f}_b$ is the external body force vector defined in section § III A; $e_t = e + \mathbf{u}\cdot\mathbf{u}/2$ is the total energy per unit mass; $e = c_v T$ is the specific internal energy. Furthermore, T is the temperature, c_v is the specific heat capacity at constant volume, and γ is the heat capacity ratio ($\gamma = c_p/c_v$), where c_p is the specific heat capacity at constant pressure. The ideal gas equation of state is employed, $p = \rho R_* T$, where $R_* = 287.05$ J/kg K is the specific gas constant of atmospheric air.

We have employed the CFD code CNS3D[12], which has been extensively validated against theoretical and computational results for shock-physics flows[13,14]. A detailed description of the numerical methods used can be found in Kokkinakis et al.[12]. In brief, CNS3D uses an upwind, Godunov-type method for the convective terms. We discretize the inter-cell numerical fluxes by solving the Riemann problem using the reconstructed values of the primitive variables at the cell interfaces. We use a one-dimensional swept unidirectional stencil for the reconstruction of the variables. The Riemann problem is solved using the so-called "Harten, Lax, van Leer, and (the missing) Contact" (HLLC) approximate Riemann solver[15].

A one-dimensional swept unidirectional stencil is used for the reconstruction of the variables. High-resolution (11$^{\text{th}}$-order) discretization is achieved in the framework of the Weighted-Essentially-Non-Oscillatory (WENO) scheme[16] with specific implementation details previously presented[12]. We briefly mention below the WENO characteristics in the framework of CNS3D. The left and right reconstruction stencils are normalized, per variable, according to a transformation function[12]. The transformation normalizes the candidate stencils so that the entire stencil's maximum value equals one. The minimum value takes a positive and nonzero value, and the value range scales relative to the maximum. Normalizing the total stencil values per variable prevents negative WENO smoothness indicator values, reduces the numerical dissipation and simplifies applying the proceeding step.

Furthermore, the WENO implementation[12] uses a total variation (TV) limiting procedure for each candidate stencil and obtains the maximum TV ratio between the candidate stencils. If all stencils contain significant discontinuities, the maximum TV ratio can be incorrectly small. Thus, an additional criterion is introduced through the linear WENO weights, i.e., the standard WENO weights are also modified according to the mapped WENO (WENO-M) approach[17].

Extensive past research has shown that the order of accuracy and the numerical design of the method used for the discretization of the convective (non-linear) terms significantly influence the accuracy of the simulations[18,19]. The above is due to the non-linearity of these terms responsible for capturing shock waves and contact discontinuities. The solution is advanced in time using a five-stage (4$^{\text{th}}$-order accurate) optimal strong-stability-preserving Runge-Kutta method[20].

III. COMPUTATIONAL PROBLEM DESCRIPTION

The computational domain is discretized using a uniform Cartesian mesh for the fireball and the indoor simulations. We performed simulations using half of the mesh resolution and found that this reduces the accuracy of the calculated forces by up to 5%. We concluded that the employed mesh resolutions provide an optimal approach regarding the accuracy and computational cost.

A. Nuclear blast simulation

The 3D fireball test case represents a 750 kT air burst detonated in the planar centre and at the height of $h_e = 2,840$ m in a domain of size 6×6×13 km (Figure 1). The computational domain is discretized using a cell size of 40 m. A symmetry boundary condition is used to model the ground and a (non-reflective) buffer layer is used for all other boundary surfaces.

The test problem is based on the superposition of heated gas representing a fireball with a standard lapse atmosphere. The only external body force is gravity, with the initial atmosphere set up to be in static equilibrium under this force. It is assumed that the ideal gas equation of state holds and that the specific heat capacities are constant for all temperatures and densities and are, therefore, calorically perfect. The lapse atmosphere is used to model the atmospheric air properties as a function of the altitude[21]:

$$\begin{aligned} T(h) &= T_0 - L_p h \\ p(h) &= p_0 \left(\frac{T(h)}{T_0}\right)^{e_x} \\ \rho(h) &= \rho_0 \left(\frac{T(h)}{T_0}\right)^{e_x - 1} \end{aligned} \tag{4}$$

where h is the altitude, $e_x = g/(L_p R_*)$ is the exponential term, the gravity is $g = 9.81$ m/s^2, standard atmospheric conditions are considered at sea level, i.e., $T_0 = 288.15$ K, $p_0 = 101,325$ Pa, $\rho_0 = 1.225$ kg/m^3, specific gas constant $R_* = 287$ J/kg·K, and finally the lapse rate $L_p = 6.5 \times 10^{-3}$ K/m. The above values are (strictly) valid up to an altitude of ∼13 km.

Moreover, the body force term in Eqs. (2) and (3) is zero in all directions except the vertical (y-direction), which is obtained according to $f_{b_y}(h) = -\mathrm{d}p(h)/\mathrm{d}h$ to ensure hydrostatic equilibrium.

An initial explosion fireball radius of $R_e = 80$ m is used, within which the internal energy of the air corresponds to the strength of the explosion considered.

B. Blast wave properties

We calculated the flow conditions behind the blast wave for the two overpressures, p_{op}, of 3 and 5 psi considered, using the below procedure.

The static pressure after the blast shock-wave is $p_s = p_0 + p_{op}$, where $p_0 = 101,325$ Pa is the standard atmospheric ambient pressure at ground level. The Mach number of the shock wave is obtained by:

$$M_s = \frac{\gamma - 1}{2\gamma} + \frac{\gamma + 1}{2\gamma}\frac{p_s}{p_0} \tag{5}$$

The velocity of the propagating shock wave and the density of the air at the shock wave are given by:

$$\mathrm{u}_s = M_s \sqrt{\gamma p_0 / \rho_0} \tag{6}$$

and

$$\rho_s = \frac{(\gamma + 1) M_s}{2 + (\gamma - 1) M_s} \tag{7}$$

The velocity of the shocked air, i.e., wind speed at the shock wave, is given by:

$$\mathrm{u}_{sa} = \mathrm{u}_s (1 - 1/\rho_s) \tag{8}$$

The pressure after the passage of the blast will gradually decay over time until it eventually drops below the atmospheric ambient pressure. The time interval from the initial pressure peak to the first recovery (ambient value) is called the positive shock duration (t_{d+}). Various empirical relations have been

developed to provide an estimate for the duration of the positive pressure of the blast pressure wave[22]. Here, we employed the following form[23]:

$$t_{d+} = 0.0012\sqrt[6]{W}\sqrt{R} \tag{9}$$

where R is the distance from the center of a spherical charge in meters (m), and W is the charge mass expressed in kilograms (kg) of TNT. The resulting value of t_{d+}, Eq. (9) is in units of seconds. The radius (meters) of the blast wave is calculated so that to give the target overpressure p_{op}[24]:

$$R = 1000\sqrt{2W^{2/3}/p_{op}} \tag{10}$$

From the various empirical relations in the literature, Eqs. (9)–(10) gave the best agreement to the simulation results of the nuclear bomb air blast scenario considered.

The exponential decay phase of the blast wave pressure front can be calculated using the modified Friedlander's equation:[25,26]:

$$p(t) = \left(1 - \frac{t}{t_{d+}}\right)\exp\left(-\frac{at}{t_{b+}}\right)p_{op} + p_0 \tag{11}$$

where the time, t, is measured from when the overpressure peak occurs, and a is a constant controlling the decay rate.

The density behind the blast wave at ground level is obtained using isentropic relations:

$$\rho(t) = p(t)\frac{\rho_0}{p_0} \tag{12}$$

Finally, the velocity of the air behind the shock is calculated as[27]:

$$u(t) = \mathrm{u}_{sa}(1-\beta t)\exp(-\alpha t) + \alpha\ln(1+\beta t) \tag{13}$$

where α and β are constants obtained from Dewey[27].

C. Rooms layout

Figure 2 shows the indoors arrangement considered in this study. The floor plan is symmetric, with the centerline going through the middle of the lower room, which permits the simulation of just half of the interior domain, thus reducing the overall computational cost.

The dimensions of the rooms, corridor, windows, and doors are given in Fig. 3. They are typical among residential buildings. For example, interior doors have 36×80 inches in width and height. The windows and doors have the same width and finish at the same height of 60 inches[28]. This gives a surface area of ∼900 square inches, which is close to the minimum net-clear opening area of 821 square inches (or 5.7 square feet) set by the 2012 International Residential Code (IRC)[29] for an egress window in residential properties.

A symmetry boundary condition is used to model the walls (slip wall), whereas all windows are set as outflow except from which the blast wave enters (inflow). The computational domain is discretized using a cell size of 3 inches.

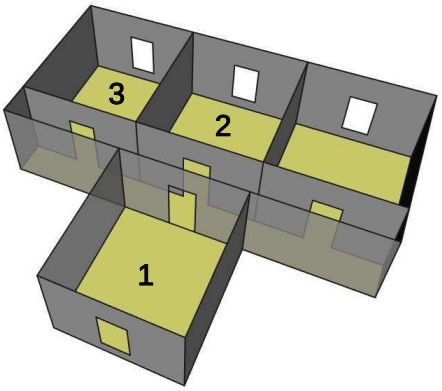

FIG. 2. Three-dimensional Illustration of the considered interior floor plan; mirror symmetry is set in the lateral direction.

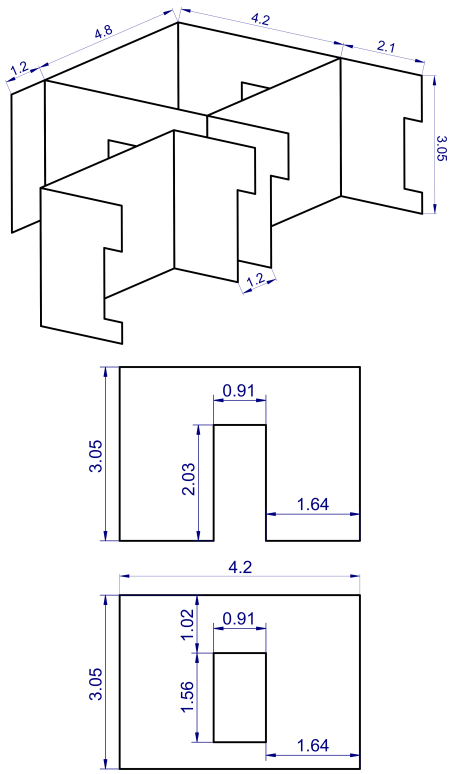

FIG. 3. Detailed schematic of the considered room layout; all dimensions in meters; top: isometric view, middle: door dimensions, bottom: window dimensions.

The shock wave enters the interior through the window of the front room (Fig. 2). According to Section § III B, at the time of the peak overpressure, at the window inlet ($t = 0$), the values of density and velocity are $\rho \approx 1.4$ kg/m^3 and $u_{sa} \approx 45.78$ m/s for an overpressure of 3 psi, and $\rho \approx 1.51$ kg/m^3 and $u_{sa} \approx 72.77$ m/s for an overpressure of 5 psi. The pressure, density and inlet velocity gradually decrease over time per Eqs. (11)–(13).

D. Wind force on human

The dynamic pressure is related to the mass airflow (gust) generated by the passing pressure wave. For example, a very high wind velocity can occur even at a slight overpressure. Dynamic pressure is highly destructive and is one of the leading causes of destruction caused by a nuclear explosion. Apart from the damage caused to buildings, the dynamic pressure can also lead to severe human injuries and fatalities.

Given the known area (A) and coefficient of drag (C_d) of some objects, it is possible to calculate the resulting force from the airflow. Here, we assume an average built person standing upright with a drag coefficient of $C_d \approx 1.3$ and a height and frontal area of 1.76 m and $\sim A_h = 0.65$ m^2, respectively, giving $C_d A_h \approx 0.84$; these values that are typical of an average human adult[30]. The force exerted by the wind is then given by:

$$F_{\text{air}} = \frac{1}{2}\rho u^2 C_d A_h \tag{14}$$

It is possible to estimate the force of the airspeed acting on a standing person at each location in the interior ($xz-$plane) using the computational results:

$$F_s = \frac{C_d}{2}\int_{y=0}^{L_y}\int_{s=s_1}^{s_2} \rho u_s |u_s|)\, \mathrm{d}s\, \mathrm{d}y \tag{15}$$

where s is a direction on the $xz-$plane. We considered the directions defined by the unit vectors $(1,0)$, $(0,1)$, $(\sqrt{1/2},\sqrt{1/2})$, and $(\sqrt{1/2},-\sqrt{1/2})$, e.g., the normal and diagonal directions (Fig. 4); u_s is the velocity in the s-direction, and ds is the computational cell's projected area on the plane normal to said direction. Finally, $L_y = 1.76$ m is the average person's height and $L_s = A_h/L_y = |s_1 - s_2|$ is the average width. The values of $s_{1,2}$ are adjusted at each location such that $L_s = A_h/L_y$ always holds.

IV. DISCUSSION

A. Nuclear explosion scenario

We simulated a nuclear blast explosion of a 750 kT atomic warhead. This detonation is a typical upper range value of a multiple independently targetable reentry vehicle (MIRV), such as, for example, the RS-28 Sarmat (Satan II)[11]. The nuclear warhead detonation is set to occur at an altitude of 2.84 km above ground to maximize the distance over which the pressure behind the blast wave has an overpressure above 5 psi[31], i.e., maximize the moderate to severe damage zone (MDZ-SDZ) to buildings in a city[3]. An illustration of the obtained explosion and resulting blast wave about 10 seconds after detonation is given in Fig. 1. The radius of the blast wave at ground level is about 4.6 km, while its peak overpressure is slightly over 7 psi.

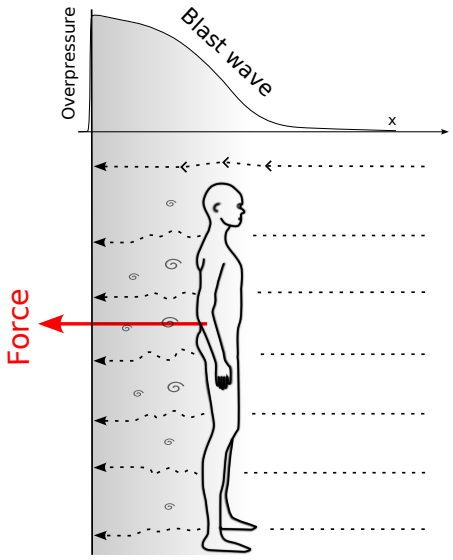

FIG. 4. Illustration of the aerodynamic drag force as per Eq. (15).

According to Glasstone and Dolan[1], the fireball size at the late stages of the explosion will be approximately twice that of the fireball's luminosity profile breakaway with time. The relationship between the maximum fireball radius and the bomb yield is thus given by:

$$R\ \ (2\times @\ \text{breakaway}) \approx 220\, W^{0.4}\ ,$$

where R is the fireball radius in feet and W is the explosion yield in kilotons TNT equivalent. For the nuclear explosion yield considered here $W = 750$ kT, $R \approx 3,108$ feet or $\sim$1.02 km. This value matches the maximum fireball radius computationally obtained when measured based on the atmospheric air heated to temperatures at and above 5,000 K.

The evolution of the blast wave is shown in Fig. 5. The upper-value limit (red color) corresponds to a maximum pressure value of 138 kPa, resulting in an overpressure of slightly over 5.3 psi. The results show the four stages of development of the spherical blast wave. In the first stage, the shock front forms as it separates from the rapid expansion of the air burst itself. In the second stage, the fully formed shock front ("incident" shock wave) travels towards the ground. Finally, a reflected wave is produced in the third stage as the incident shock wave reflects from the ground. For a smooth surface,

the total reflected overpressure in the region near ground zero will be more than twice the value of the peak overpressure of the incident blast wave. Note that the reflected wave travels through atmospheric air heated and compressed by the incident wave. As a result, the reflected wavefront moves faster than the incident wave and, under certain conditions, overtakes it so that the two wavefronts eventually merge to produce a single wavefront, called the "Mach stem". In Fig. 5, the Mach stem remains relatively small due to the explosion parameters considered. The above results and analysis also agree with the observations of Glasstone and Dolan[1].

During the earlier time instants shown in Fig. 5, the pressure behind the blast wave is significantly higher, as evidenced by the saturation of the corresponding color (red). However, even 5 km from the explosion epicentre, the overpressure remains slightly above 5 psi (36.7 kPa). The thermal radiation emitted from such a nuclear explosion would be sufficient to cause third-degree burns (severe scarring or disablement, amputation) up to 10.7 km away[31]. Moreover, since thermal radiation travels at the speed of light, its effect would be felt instantly and before the blast wave. Thus, the intense wind speeds behind the blast wave would also intensify and spread fires.

Typically, overpressures of 5 psi cause moderate blast damage, e.g., most residential (timber) buildings collapse, injuries are universal, and fatalities are widespread. On the other hand, overpressures of 3 psi are estimated to lead to light and moderate damages in cities[3]. Buildings are damaged between 2 and 5 psi, primarily due to the abrupt rise in the air velocity following the blast shock wave impact (Fig. 6). Though such overpressures are not sufficiently high to harm humans directly, despite the abrupt pressure rise, high-speed winds behind the blast wave can injure humans and cause fatalities. At an overpressure of 1 psi, glass windows may be partially damaged. At the overpressures of 3 and 5 psi considered here, most residential building windows will shutter instantly[3], and the blast wave is assumed to travel through the window unobstructed. Most residential buildings will not structurally withstand the wind speeds associated with higher overpressures and, thus, are not within the scope of the present study.

B. Indoors hazard

We examined the effect of the airspeed entering through a single window of an indicative indoor arrangement to establish the severity of danger to humans.

Within the MDZ, the high-wind speeds behind the blast wave are one of the principal destruction mechanisms. The effects of wind at different velocities are described below:

- 50 mph (22.35 m/s): raindrops begin to hurt; bending or leaning forward is required to stay balanced; large trees can be blown down.
- 70 mph (31.3 m/s): maximum wind speed most humans can withstand without getting blown away; can blow down some street signs and power lines; cars start rocking and potentially flip.
- 100 mph (44.7 m/s): The force exerted by the wind on a human is almost equivalent to the gravitational pull of the earth, e.g., the equivalent of walking up a vertical wall; unlikely not to be blown away unless grabbing onto a firm object or hiding behind it; capable of moving most cars.
- 120+ mph (53.65 m/s), staying upright is no longer possible.

For indoor skydiving, wind tunnels are used to create artificial winds of 100-130 mph (∼44.7-58.1 m/s) to keep a person facing head-on (face down in this case) "afloat" in the air against the pull of gravity.

Figure 7 shows the 3D contours of the maximum airspeed attained. The highest speed is at the window and door of the front room (room 1), where the blast wave enters the space (Fig. 2). At an overpressure of 3 psi, the maximum internal airspeed is slightly over 140 m/s, whereas at 5 psi, it is slightly over 184 m/s. The short time over which the high-speed winds occur does not allow sufficient time to take a protective stance, e.g., lean forward, bend, lie flat on the floor, etc. Sustaining wind speeds of 140 m/s for about one second would lift and throw most humans off the ground.

The results show that the maximum indoor air velocities are much higher compared to the airspeed entering through the window, i.e., the blast wave peak wind velocities (outdoors) are 46 and 73 m/s at 3 and 5 psi overpressures, respectively, while the indoor peak velocities are 140 m/s and 184 m/s, respectively. The physical mechanism responsible for the increased interior wind speed is the sudden expansion of the shock through the front room window. The density of the shocked air behind the blast wave is higher than the local ambient value. Therefore, despite the shock's expansion process, the shock air density is around the ambient value. As a result, the effect of the dynamic pressure at such wind speeds indoors is comparable to the impact of the naturally occurring high-speed winds outdoors. An essential difference is a duration over which the high-speed wind will last. Nonetheless, despite the shorter time of the high-speed wind behind the blast wave, the imparted force still remains substantial.

Moreover, high airspeed would accelerate flying debris picked up by the blast wave outdoors and pieces from the shuttered window. Therefore, numerous high-speed projectiles will impact the room as the blast wave develops after entering the room. In black powder muskets, firearm muzzle velocities range from approximately 120 m/s to 370 m/s. Therefore, any solid debris travelling anywhere near such wind speeds has the potential to cause severe injury or fatalities.

By applying the methodology of Section § III D in conjunction with the computational results, we can estimate the maximum (aerodynamic) force exerted on an average weight person, approximately 80 kg[32,33], during the first 10 seconds after the blast wave enters. This allows the creation of a simple map indicating which indoor areas are hazardous. We use the gravitational force to normalize the wind force and plot the contour surface of the normalized force in Fig. 4. Areas at which the force exerted equals that of the gravitational force, $F_g = mg$, are in yellow, indicating the potential hazard

Accepted to Phys. Fluids 10.1063/5.0132565

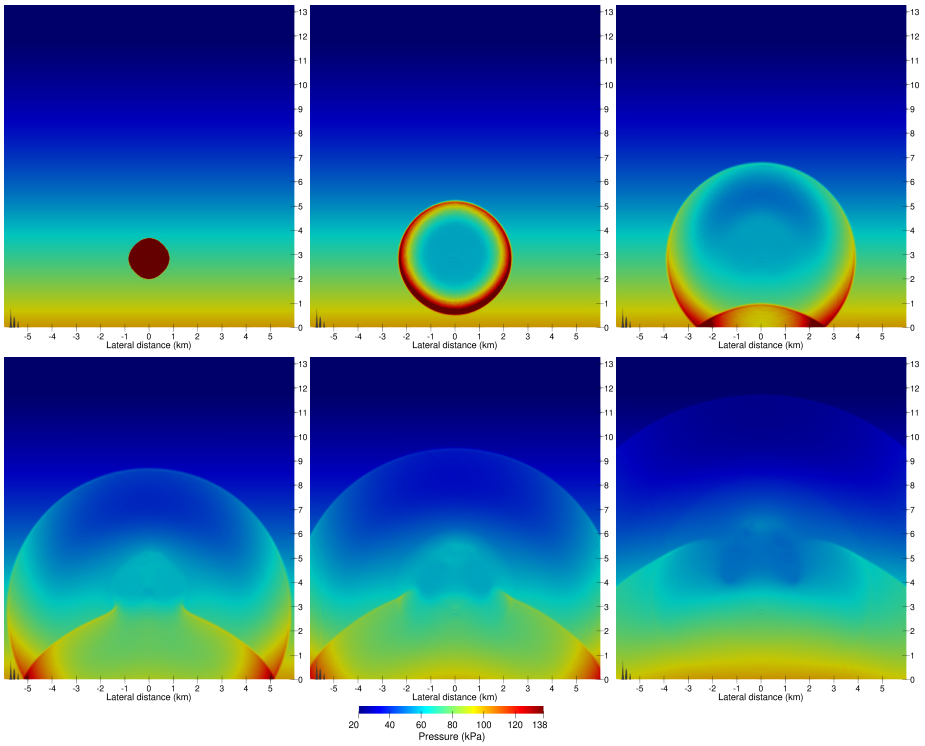

FIG. 5. Two-dimensional contour plots of the shock wave evolution following the 750 kT detonation of a nuclear warhead; x and y axes are the ground distance and altitude in units of km; seconds after initial blast from left-to-right and top-to-bottom: 0.6, 2.8, 6.7, 12.0, 14.4, and 21.1.

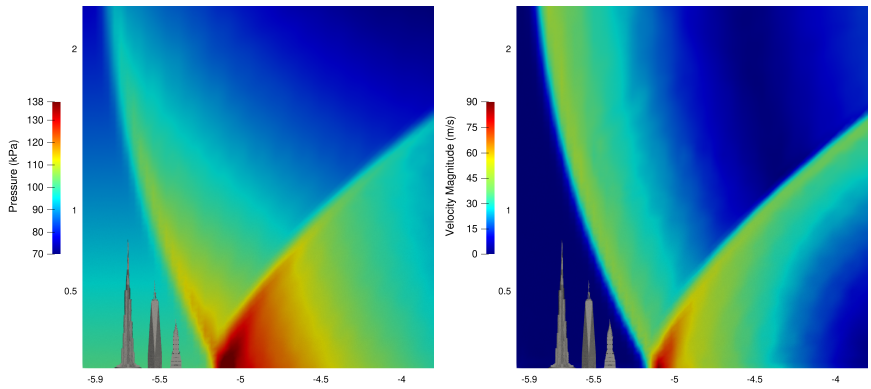

FIG. 6. Two-dimensional contour plots of the pressure and airspeed generated behind the shock wave ~ 12 seconds after the detonation of a 750 kT nuclear warhead; $x-$ and $y-$ axis are the ground distance and altitude in units of km; skyscrapers depicted for reference are from right-to-left the Chrysler building, the One World Trade Center, and the Burj Khalifa.

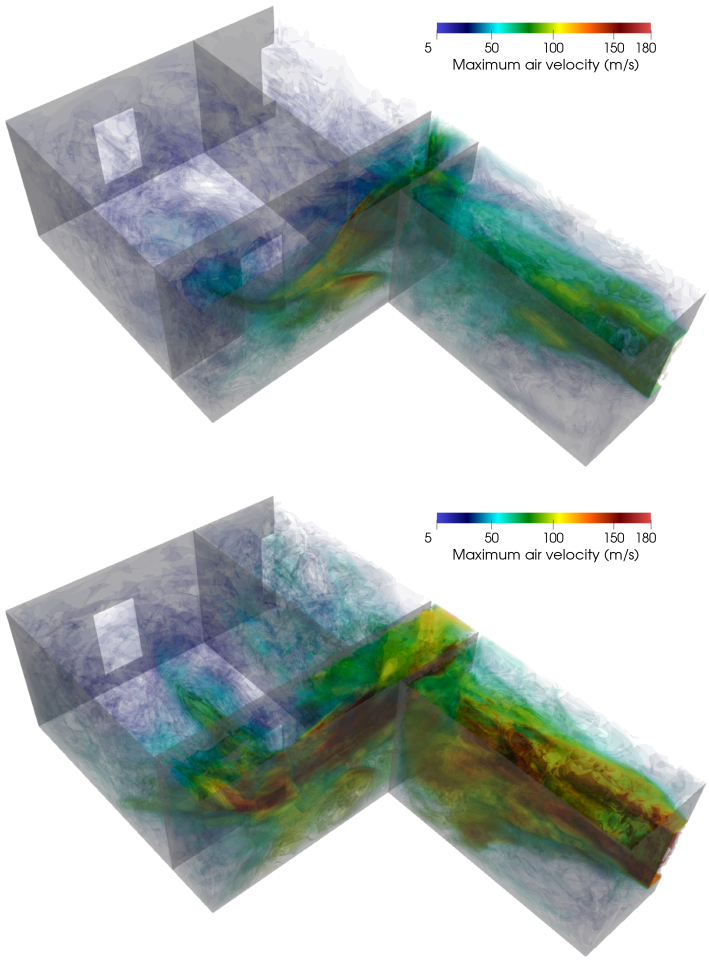

FIG. 7. Contours of the maximum airspeed attained during the first 10 seconds after the blast wave enters the window; overpressure of (top) 3 psi, and (bottom) 5 psi.

of losing balance and falling over. Forces around $F/F_g \approx 0.5$, green-colored areas, would remain hazardous, particularly for people weighing less than the average weight. Values of 5 and above, red colored areas, would be extremely hazardous, with values above 10 reflecting stronger than hurricane forces being exerted. Such regions practically guarantee that humans would be violently pushed and thrown over. Most of the force is applied in less than half a second (Fig. 9). Using the data of Fig. 9, it is estimated that in the worst-case scenario and for the overpressure of 3 psi, an average-weight person standing in the corridor could be pushed about 10 meters within less than a second, excluding surface friction and any change in the person's stand within that time. In the front room (room 1), the same person would be thrown about 9.5 meters; in room 2, over 2.2 meters; in room 3, around (approximately) 1.7 meters. For an overpressure of 5 psi, and in the worst case scenario, the average weight person could be thrown at a distance of 21 meters in room 1, 8.5 meters in room 2, 3.3 meters in room 3, and 20 meters in the corridor.

Due to the rooms' dimensions, humans will not be ejected

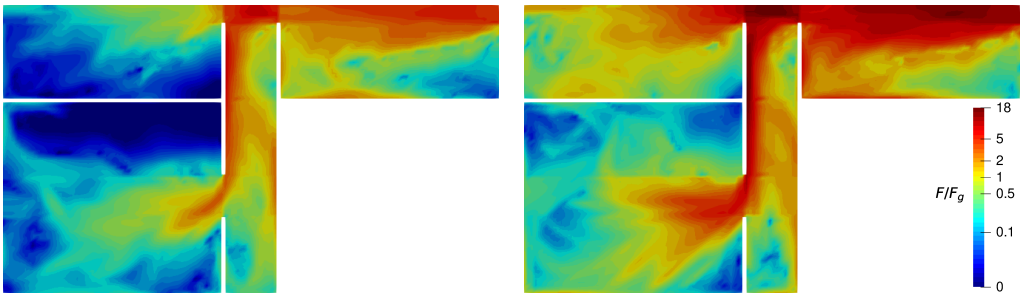

FIG. 8. Contours of the maximum air force (as a multiple of the gravitational body force) applied to an average person during the first 10 seconds after the blast wave enters the window; results for overpressures of 3 psi and 5 psi are shown in the left and right plots, respectively.

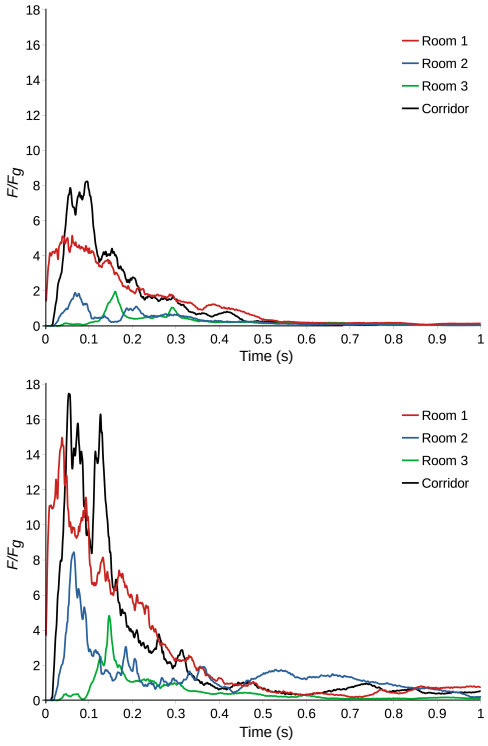

FIG. 9. Plot of the maximum air force (as a multiple of the gravitational body force) versus time applied to an average person during the first 10 seconds after the blast wave enters through the window; overpressure of (top) 3 psi, and (bottom) 5 psi.

such a large distance. Instead, they will be thrown with great force to the walls. In rooms 2 and 3, however, the force generated at 5 psi is sufficient to throw a person standing near the door out of the window. Otherwise, the impact on a solid surface will cause severe injury or death. Regarding critical indoor regions, the most dangerous locations are the corridor, near the doors, and particularly the front room area. At 5 psi, the critical region extends into room 2.

The acceleration is also significant. For example, at an overpressure of 3 psi, the acceleration is 50 g's in room 1 and 80 g's in the corridor. At 5 psi, the acceleration exceeds 140 g's. People can survive accelerations over 18 g's momentarily and even withstand up to 35 g's and still survive, as was demonstrated in the mid-1950s[34,35]. In the same experiments, a (trained) test subject withstood 46.2 g's over 1.1 seconds and was (surprisingly) still able to walk away unscathed. In another experiment, a person endured a whopping 40 g's (albeit for 0.04 seconds) with a peak value of 83 g's during a nearly instantaneous stop[36]. The person walked away from the experiment without any side effects. Thus, despite the violent accelerations involved, the experiments show that the human body can handle massive g-loads, but only when subjected to them for a very short time.

V. CONCLUSIONS

We studied the impact of a nuclear blast corresponding to a 750 kT atomic warhead on humans indoors in a nuclear explosion's moderate damage zone (MDZ). MDZ is the area where concrete buildings may not collapse. At distances featuring overpressures of 5 psi, severe injuries and fatalities will be widespread, and damage to heavy structures will occur. At longer distances featuring an overpressure of 3 psi, severe human injuries and the destruction of smaller built-in structures will occur.

The study revealed that the airspeed behind the blast wave induces significant forces on humans indoors. The most potent forces are experienced for a short period of up to half a second. The airspeed behind the blast wave accelerates indoors to even higher velocities. This stems from the expan-

sion of the shock waves entering the space through an opening such as a window. Furthermore, channelling effects can further accelerate the air in the corridors.

The force hitting a standing person indoors is equivalent to several $g-$forces of body mass acceleration and could lift a person off the ground and throw them to the walls. At an overpressure of 3 psi, the acceleration can reach 80 g's, while at 5 psi, the acceleration exceeds 140 g's. However, there are areas inside the rooms where the airspeed and the associated forces are reduced. The simulations provide colored maps of the indoor areas where the risk of human injury is reduced.

Given the findings, the relevant authorities could issue instructions to prevent the nuclear blast from impacting humans situated indoors from the exposure to high-speed winds behind the incoming blast waves. Moreover, the results could guide the future design of concrete structures.

DATA AVAILABILITY

The data that support the findings of this study are available from the corresponding author upon reasonable request.

REFERENCES

[1]S. Glasstone and P. J. Dolan, "The effects of nuclear weapons," Tech. Rep. Third edition (Department of Defense; Department of Energy, Washington, D.C. (USA), 1977).
[2]G. F. Kinney and K. J. Graham, *Explosive Shocks in Air* (Springer Berlin Heidelberg, Berlin, Heidelberg, 1985).
[3]Federal Emergence Management Agency (FEMA), "Planning guidance for response to a nuclear detonation," Tech. Rep. Third edition (U.S. Department of Homeland Security, 2022) https://www.fema.gov/sites/default/files/documents/fema_nuc-detonation-planning-guide.pdf.
[4]B. E. Moroz, H. L. Beck, A. Bouville, and S. L. Simon, "Predictions of dispersion and deposition of fallout from nuclear testing using the noaa-hysplit meteorological model," Health physics **99**, 252–269 (2010).
[5]J. C. Schofield, *Mapping Nuclear Fallout Using the Weather Research & Forecasting (WRF) Model*, Theses and dissertations, Air Force Institute of Technology (AFIT) (2012), 1188.
[6]R. E. Marrs, "Radioactive fallout from terrorist nuclear detonations," Tech. Rep. UCRL-TR-230908 (Lawrence Livermore National Laboratory, 2007).
[7]G. C. Benjamin, M. McGeary, and S. R. McCutchen, eds., *Assessing Medical Preparedness to Respond to a Terrorist Nuclear Event: Workshop Report*, Institute of Medicine (US) Committee on Medical Preparedness for a Terrorist Nuclear Event (National Academies Press (US), Washington (DC), 2009).
[8]M. Levi, *On Nuclear Terrorism* (Harvard University Press, Cambridge, MA and London, England, 2021).
[9]G. Rolph, F. Ngan, and R. Draxler, "Modeling the fallout from stabilized nuclear clouds using the hysplit atmospheric dispersion model," Journal of Environmental Radioactivity **136**, 41–55 (2014).
[10]E. W. Bierly and A. W. Klement, "Radioactive fallout from nuclear weapons tests," Science **147**, 1057–1060 (1965).
[11]A. Genys, "RS-28 Sarmat," Accessed: 2022-10-18.
[12]I. Kokkinakis, D. Drikakis, K. Ritos, and S. M. Spottswood, "Direct numerical simulation of supersonic flow and acoustics over a compression ramp," Physics of Fluids **32**, 066107 (2020).
[13]M. Hahn, D. Drikakis, D. L. Youngs, and R. J. R. Williams, "Richtmyer–Meshkov turbulent mixing arising from an inclined material interface with realistic surface perturbations and reshocked flow," Phys. Fluids **23** (2011), 10.1063/1.3576187.
[14]A. Bagabir and D. Drikakis, "Numerical experiments using high-resolution schemes for unsteady, inviscid, compressible flows," Computer Methods in Applied Mechanics and Engineering **193**, 4675–4705 (2004).
[15]E. F. Toro, M. Spruce, and W. Speares, "Restoration of the contact surface in the HLL-Riemann solver," Shock Waves **4**, 25 – 34 (1994).
[16]D. S. Balsara and C.-W. Shu, "Monotonicity preserving weighted essentially non-oscillatory schemes with increasingly high order of accuracy," Journal of Computational Physics **160**, 405 – 452 (2000).
[17]A. K. Henrick, T. D. Aslam, and J. M. Powers, "Mapped weighted essentially non-oscillatory schemes: Achieving optimal order near critical points," Journal of Computational Physics **207**, 542 – 567 (2005).
[18]F. Grinstein, L. Margolin, and W. Rider, eds., *Implicit Large Eddy Simulation: Computing Turbulent Fluid Dynamics* (Cambridge University Press, 2007).
[19]K. Ritos, I. W. Kokkinakis, D. Drikakis, and S. M. Spottswood, "Implicit large eddy simulation of acoustic loading in supersonic turbulent boundary layers," Physics of Fluids **29**, 046101 (2017).
[20]R. Spiteri and S. Ruuth, "A new class of optimal high-order strong-stability-preserving time discretization methods," SIAM Journal on Numerical Analysis **40**, 469–491 (2002).
[21]E. Houghton, P. Carpenter, S. H. Collicott, and D. T. Valentine, *Aerodynamics for Engineering Students*, 6th ed. (Butterworth-Heinemann, Boston, 2013).
[22]A. Ullah, F. Ahmad, H.-W. Jang, S.-W. Kim, and J.-W. Hong, "Review of analytical and empirical estimations for incident blast pressure," KSCE Journal of Civil Engineering **21** (2017), 10.1007/s12205-016-1386-4.
[23]M. Sadovskiy, "Mechanical effects of air shockwaves from explosions according to experiments," in *Selected Works: Geophysics and Physics of Explosion* (Nauka Press, Moscow, Russia, 2004).
[24]M. Held, "Blast waves in free air," Propellants, Explosives, Pyrotechnics **8**, 1–7 (1983).
[25]J. Henrych, *The Dynamics of Explosion and Its Use* (Elsevier Scientific Publishing Company, Amsterdam and New York, 1979) p. 562.
[26]W. Baker, P. Cox, J. Kulesz, R. Strehlow, and P. Westine, *Explosion Hazards and Evaluation* (Elsevier Science, 1983) p. 840.
[27]J. M. Dewey, "The air velocity in blast waves from t.n.t. explosions," Proc. R. Soc. Lond. A **279**, 366–385 (1964).
[28]Bhushan Mahajan, "What is standard window size," https://civiconcepts.com/blog/standard-window-size (2019-2022), [Online; accessed 21-October-2022].
[29]https://codes.iccsafe.org/content/IRC2012P13.
[30]J. F. R. McIlveen, "The everyday effects of wind drag on people," Weather **57**, 410–413 (2002).
[31]A. Wellerstein, "Nukemap," Accessed: 2022-10-18.
[32]S. C. Walpole, D. Prieto-Merino, P. Edwards, J. Cleland, G. Stevens, and I. Roberts, "The weight of nations: an estimation of adult human biomass," BMC Public Health **12**, 439 (2012).
[33]Wikipedia contributors, "Human body weight — Wikipedia, the free encyclopedia," https://en.wikipedia.org/w/index.php?title=Human_body_weight&oldid=1096037841 (2022), [Online; accessed 21-October-2022].
[34]J. P. Stapp, "Effects of mechanical force on living tissues. I. Abrupt deceleration and windblast," The Journal of aviation medicine **26**, 268–288 (1955).
[35]C. D. Hughes and J. P. Stapp, "Effects of mechanical force on living tissues. II. Supersonic deceleration and windblast," The Journal of aviation medicine **27**, 407–413 (1956).
[36]N. R. Council, *Impact Acceleration Stress: A Symposium* (The National Academies Press, Washington, DC, 1962).

PLEASE CITE THIS ARTICLE AS DOI: 10.1063/5.0132565

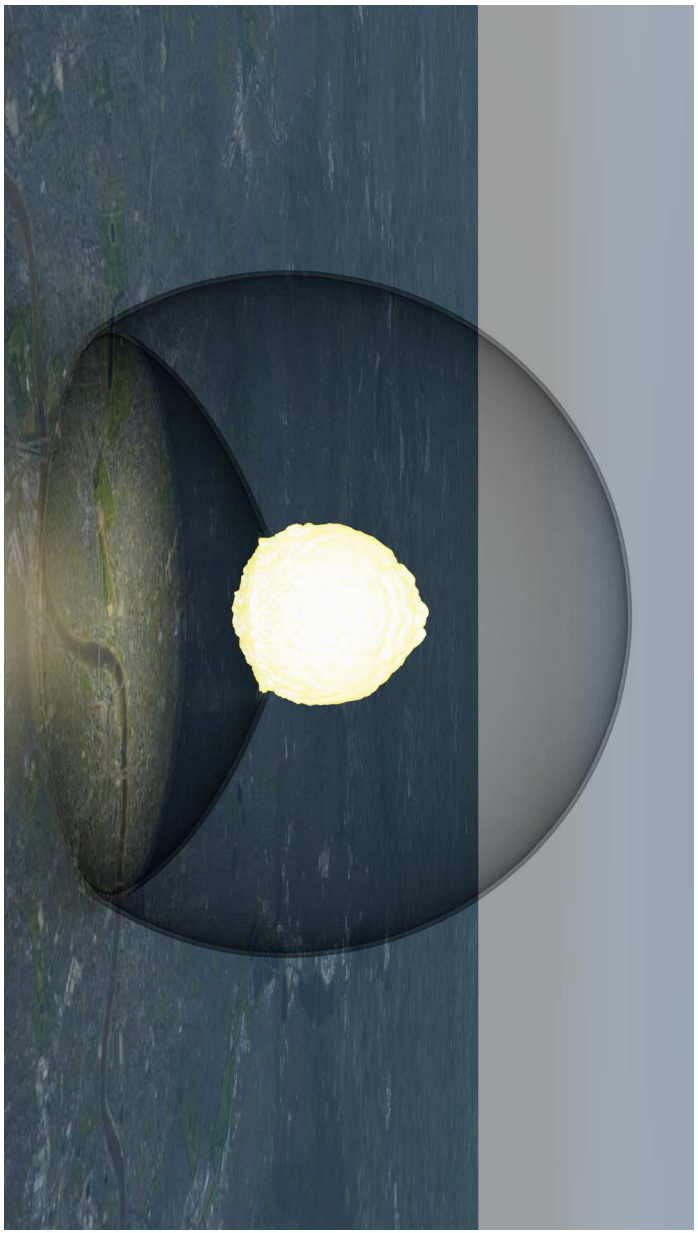

Physics of Fluids

PLEASE CITE THIS ARTICLE AS DOI: 10.1063/5.0132565

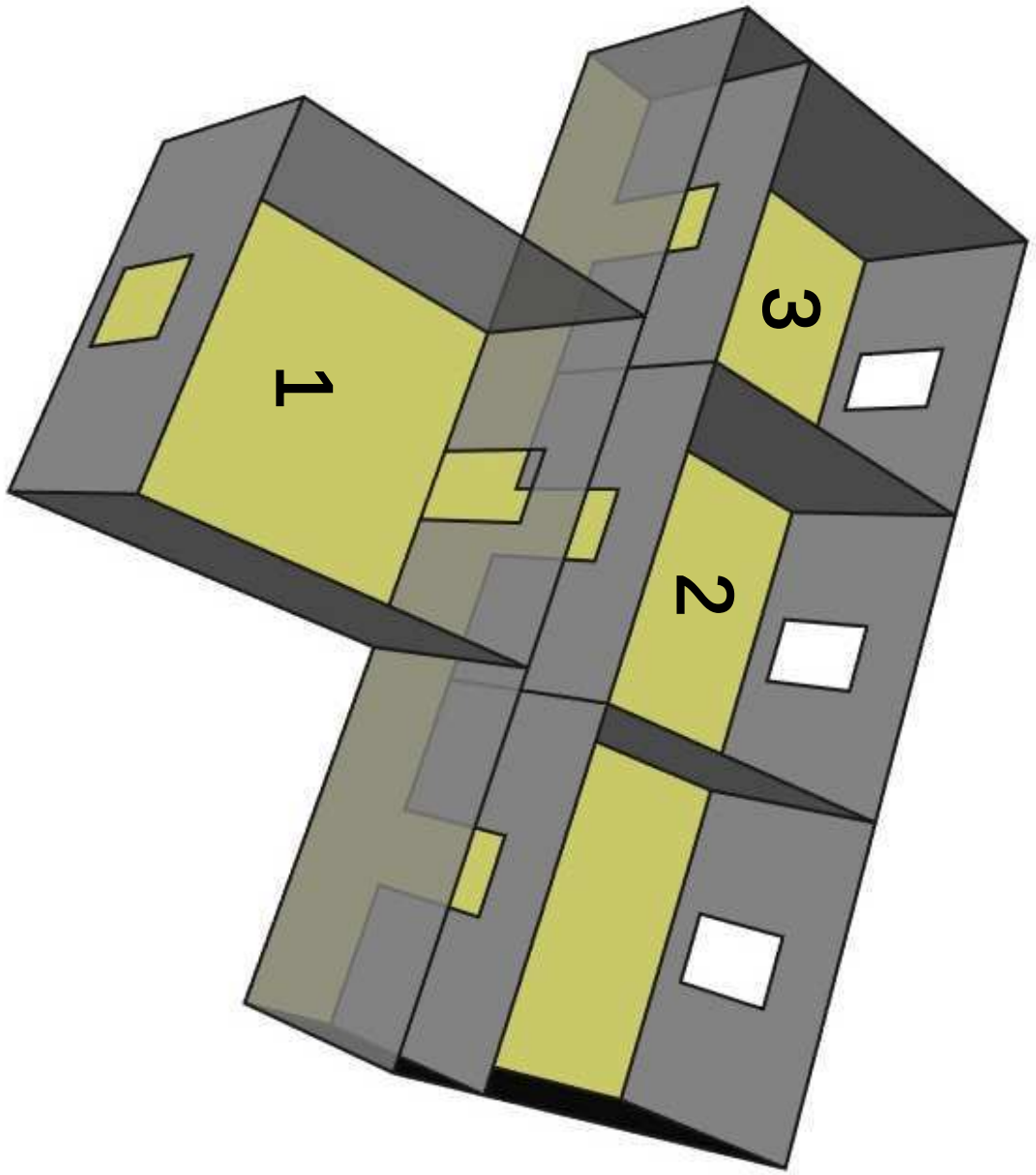

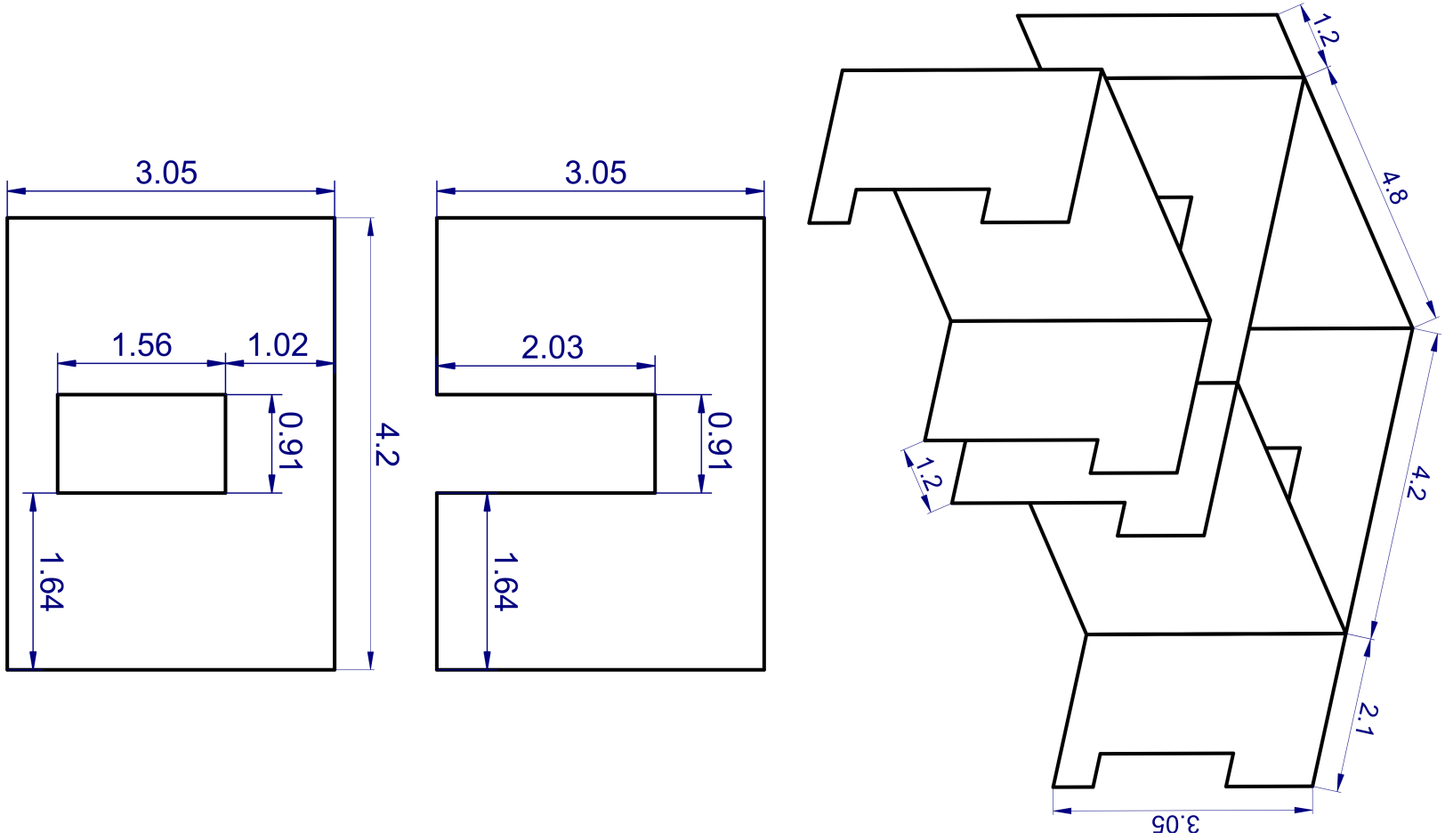

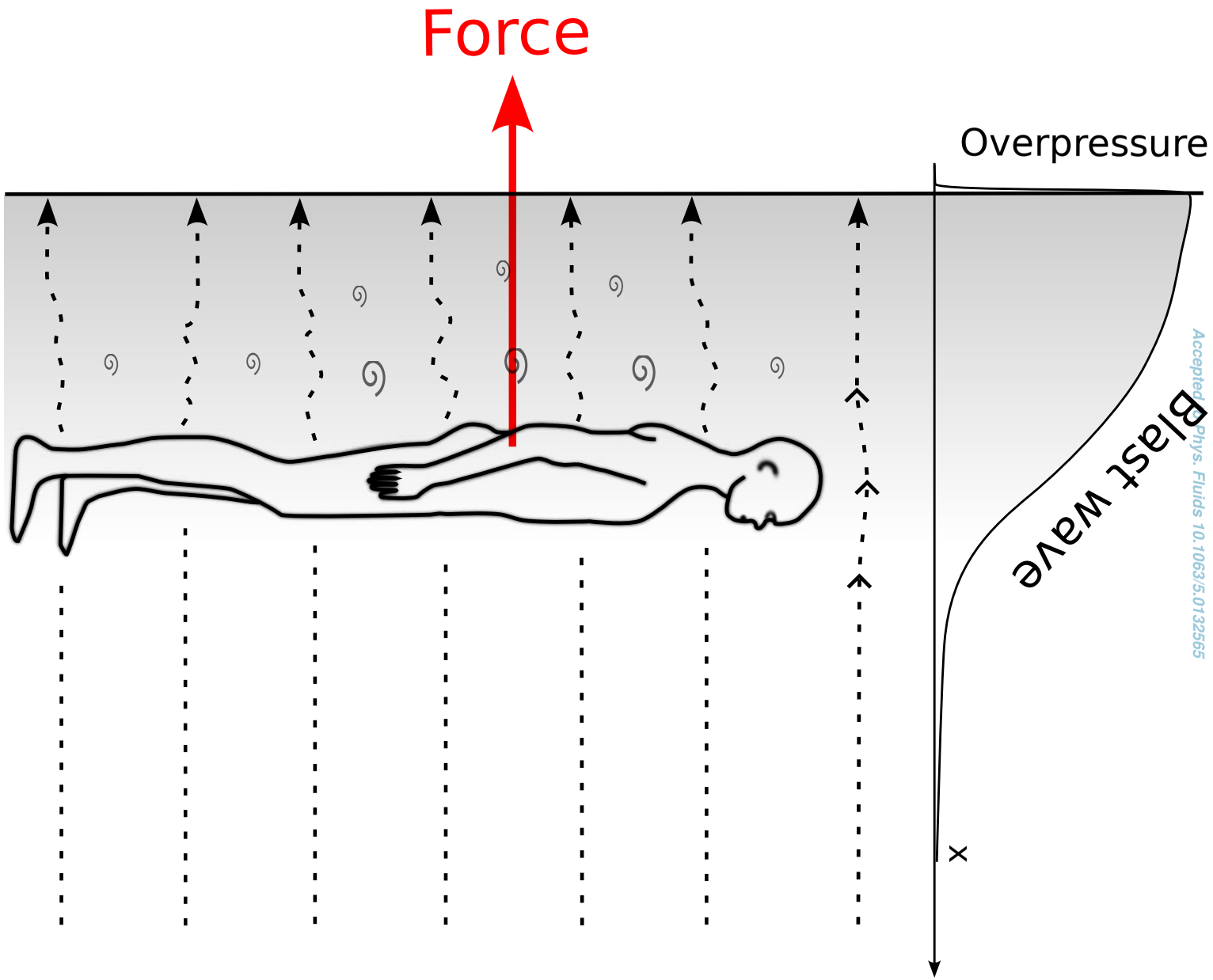

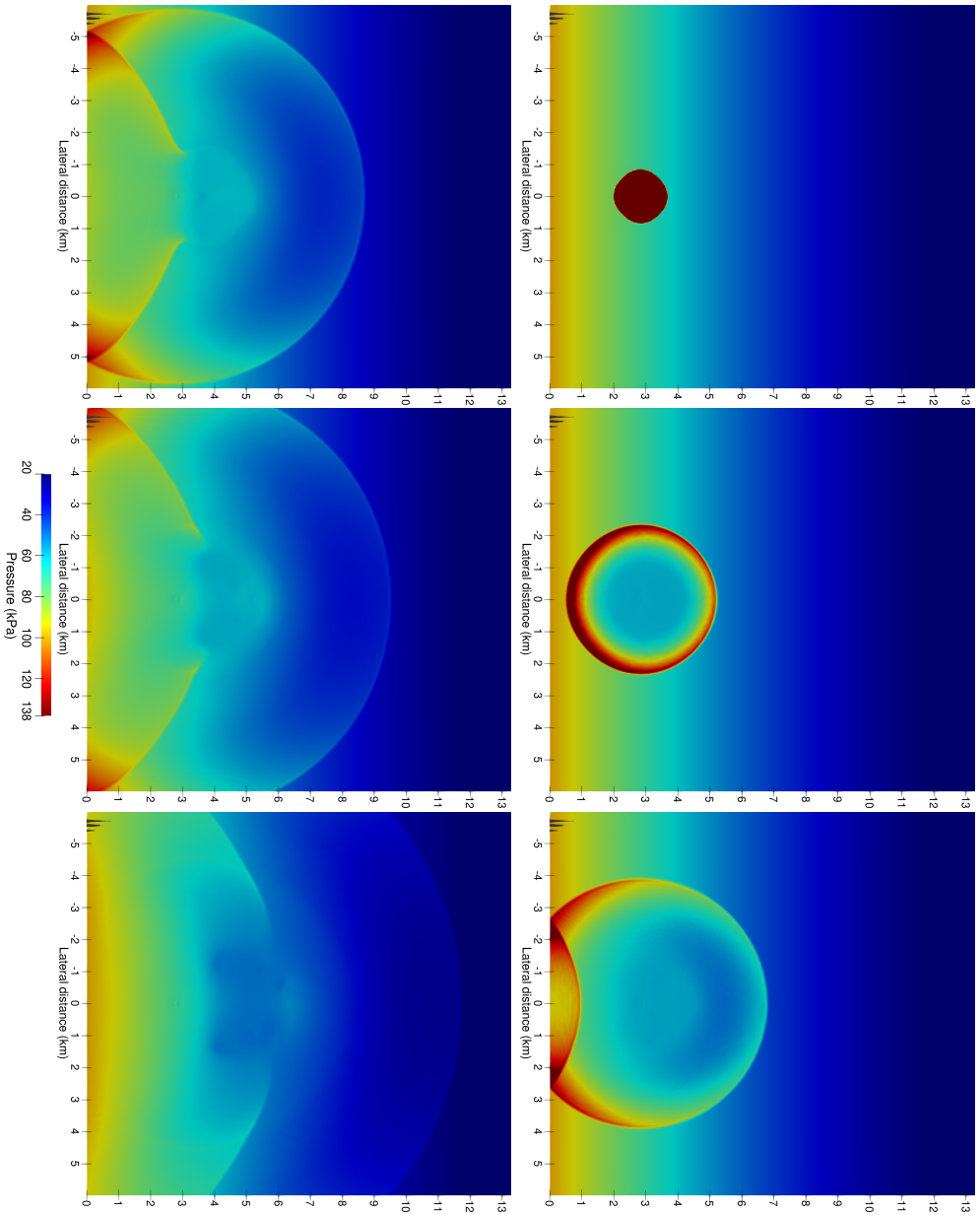

PLEASE CITE THIS ARTICLE AS DOI: 10.1063/5.0132565